Progress In Electromagnetics Research C, Vol. 67, 11–20, 2016

A Wide Spectrum Sensing and Frequency Reconfigurable Antenna for Cognitive Radio

Sonia Sharma* **and Chandra C. Tripathi**

Abstract—A novel hybrid antenna capable of both spectrum sensing and frequency reconfigurability is proposed in this paper. The proposed hybrid antenna senses spectrum over a wide frequency range from 1 GHz–12 GHz and accordingly reconfigures its operating frequency in any of the four different frequencies, i.e., 2.1 GHz, 2.96 GHz, 3.5 GHz and 5 GHz. Since wideband response for spectrum sensing and each frequency state works independently, there is no interference among various signals. The wideband response for spectrum sensing is obtained by exciting semicircular arc having staircase-shaped slot in the ground plane. Frequency reconfiguration is achieved by electronic switching among various matching stubs. Both simulated and experimental results for the return loss, gain and radiation patterns are presented. The proposed hybrid antenna shows a measured return loss better than −20 dB in all the operating bands, a bidirectional radiation pattern and 4.8 dB gain in $\theta = 20^\circ$ and 120° in E plane.

1. INTRODUCTION

In recent years, due to rapid proliferation of wireless communications systems, the limited electromagnetic spectrum has become more and more congested. On the other hand, it is generally recognized that the spectrum is idle for 90% of the time [1–3]. The under utilization of the frequency spectrum has been inspiring the use of Reconfigurable Radio concepts, such as Cognitive Radio (CR). The CR senses the spectrum and reconfigures itself to optimize its operation for more efficient communications and spectrum use [3–5].

The CR system is integrated with two types of antennas: ultra wideband (UWB) antenna as a spectrum sensor and reconfigurable antenna for multiple communication. However, the integration of multiple antennas for CR into a limited space without disturbing the characteristics of individual antenna is quite challenging. In literature, a number of antennas are reported which effectively integrated wideband and narrowband designs without degrading the overall performance [5–11]. In all the reported work, spectrum sensing antenna is implemented by large sized UWB printed monopole patch with various shapes, such as circle [6], rectangle [7, 8], bevel [9], Vivadi [10], etc., and excited by either CPW or microstrip feed line. In these UWB designs, narrowband antennae are integrated by a number of ways, such as inserting reconfigurable filter in the feed line [6], tuning the antenna using open stub [8], utilizing some part of large ground plane as a narrowband radiator [9], utilizing the space between two taper slots [10], inserting a small sized narrowband antenna at a point where electric field does not disturb the coplanar waveguide (CPW) UWB antenna [11], etc.

In most of the designs, the numbers of frequency reconfiguration states are limited because of size constraint of the overall structure. Moreover, either lumped or microstrip-based matching network is added to match the narrowband antenna at primary frequency, and then extra matching circuitry is needed to make the design frequency reconfigurable. In these designs, frequency switching is realized

Received 8 July 2016, Accepted 3 August 2016, Scheduled 26 August 2016

* Corresponding author: Sonia Sharma (sonia990@gmail.com).

The authors are with the Department of Electronics and Communication Engineering, UIET, Kurukshetra University, Kurukshetra, India.

by using PIN diodes [8, 12], varactors [6], field effect transistor (FET) switches [13]. The frequency reconfigurable operation demands increase in a number of frequency states, hence higher number of switches together with their biasing elements are needed resulting in increase in total cost and design complexity. So, further upgradation of these antennas to increase the reconfiguration states is quite challenging because of space constraints on board. This may compromise the goal of combining the wideband and reconfigurable narrowband antennas for CR systems. Therefore, in this work, UWB antenna and reconfigurable antenna are integrated so that they do not disturb the characteristics of each other. The proposed design facilitates further upgradation of antenna to increase the number of frequency states by simply redesigning the matching stubs for intended frequencies.

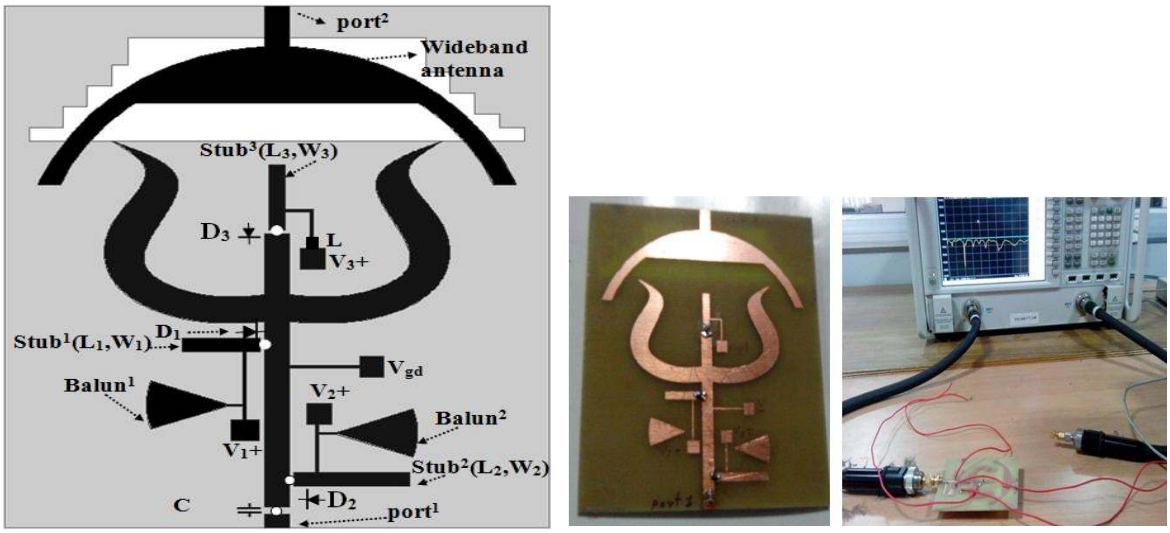

(a) (b)

Figure 1. (a) Layout of hybrid antenna. (b) Fabricated prototype and experimental setup.

A combination of spectrum sensing and frequency reconfigurable antenna design for cognitive radio is presented here and shown in Fig. 1. The proposed hybrid antenna can sense the spectrum from 1 GHz–12 GHz by a semicircular arc with slotted ground type antenna structure. After recognizing the spectrum condition, the proposed antenna can reconfigure its frequency in 3.5 GHz, 5 GHz, 2.96 GHz, 2.1 GHz states depending on the control state of PIN diode (BAR64-02). The most attracting feature of proposed design is its ability to work independently for spectrum sensing and switching over frequency reconfigurable states, making it more robust against power fluctuations and intra-band interferences. The proposed antenna reduces the number of antennas for CR because spectrum sensing and frequency reconfiguration are achieved in a single design. So the proposed hybrid antenna has a compact design which is well suitable for CR application [1, 2] to use spectrum efficiently.

This paper is organized as follows. First, we describe the design evolution in Section 2. Section 3 describes the design layout and experimental setup. Simulated and measured results for the proposed hybrid antenna are elaborated in Sections 4 and 5, respectively. Finally, the work is concluded in Section 6.

2. DESIGN EVOLUTION

The final hybrid antenna is designed in a sequential way as follows. Firstly, a simple antenna is designed at 3.5 GHz as shown in Fig. 2(a). The motivation of the present shape is to reduce the antenna size at low frequency. Some design innovation has been done to bend the antenna length so that it not only produces single resonating frequency, but also reduces the antenna size significantly. Fig. 2(b) shows its fabricated prototype, and Fig. 2(c) shows the E-field distribution. Fig. 3(a) shows that the

antenna's simulated resonating frequency is 3.49 GHz with $S_{11} = -22.5$ dB whereas the measured value is found at 3.46 GHz with $S_{11} = -28.71$ dB. The minor shift in measured value is due to imperfection in fabrication process. In simulation, the antenna shows an input impedance of 52 Ω and Voltage Standing Wave Ratio (VSWR) of 1.24 as indicated in Fig. 3(b).

The design is extended by imprinting a UWB arc above the simple antenna. Structure of the proposed UWB antenna is basically developed from conventional cone-disc UWB antenna shape. The semicircular arc type structure is excited by microstrip feed, and impedance matching is done by cutting rectangular slots in the ground plane. Further, the impedance bandwidth is enhanced by modifying the slot shape into staircase type by cutting rectangular slot at specific position as shown in Fig. 4.

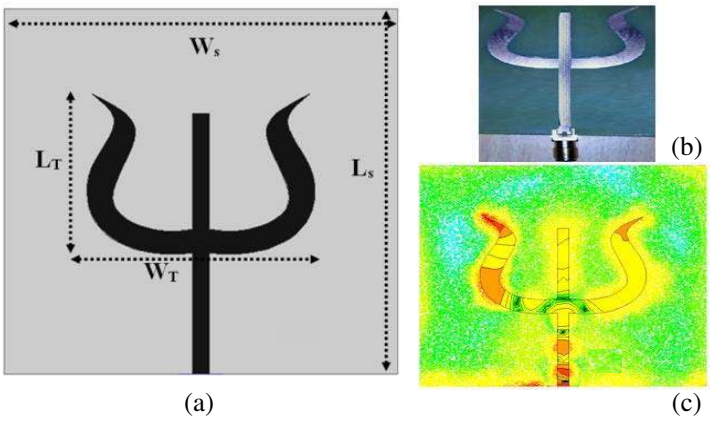

Figure 2. (a) Layout of simple antenna. (b) Fabricated prototype. (c) E field distribution.

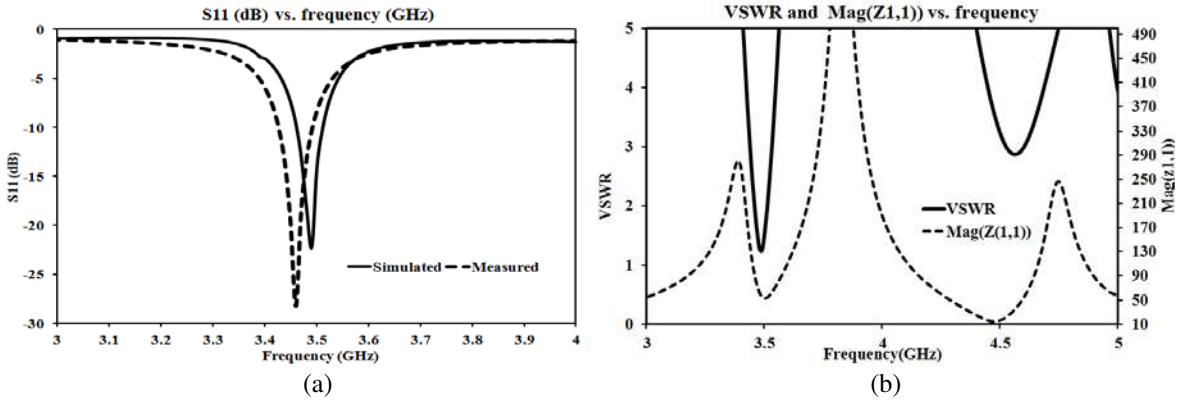

Figure 3. (a) S_{11} vs. frequency. (b) VSWR and impedance vs. frequency of simple antenna.

Now to achieve the frequency reconfiguration in the proposed antenna, microstrip open stubs are placed at proper position, so that these stubs match the antenna's input impedance at different frequencies. At the center frequency 3.5 GHz, the input impedance was determined from the simulations, and this impedance was transferred along the 50 Ω microstrip feed line to the point where the impedance had a real part of 50 Ω and a random imaginary part. At that point, an open circuit microstrip stub[1] was placed parallel to the microstrip feed line to cancel the imaginary part. Now to match the antenna at the second frequency, the impedance at the input port was determined by simulation when the first matching stub is in place (not attached with the feed line) so that the antenna should be optimally matched using stub[2].

It should be noted that after fixing the dimension of one stub for a fixed frequency band, in some cases, if other parameters are changed, all the frequency bands are affected, and the antenna needs

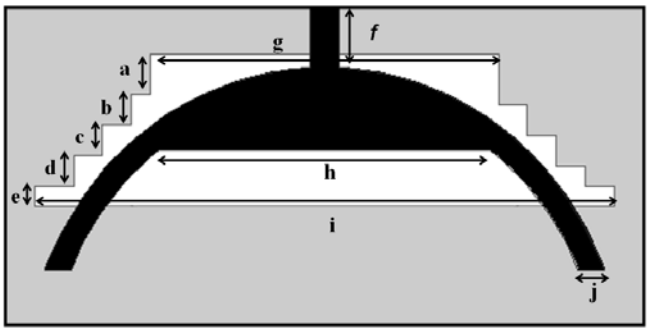

Figure 4. Semi circular arc type structure for UWB operation.

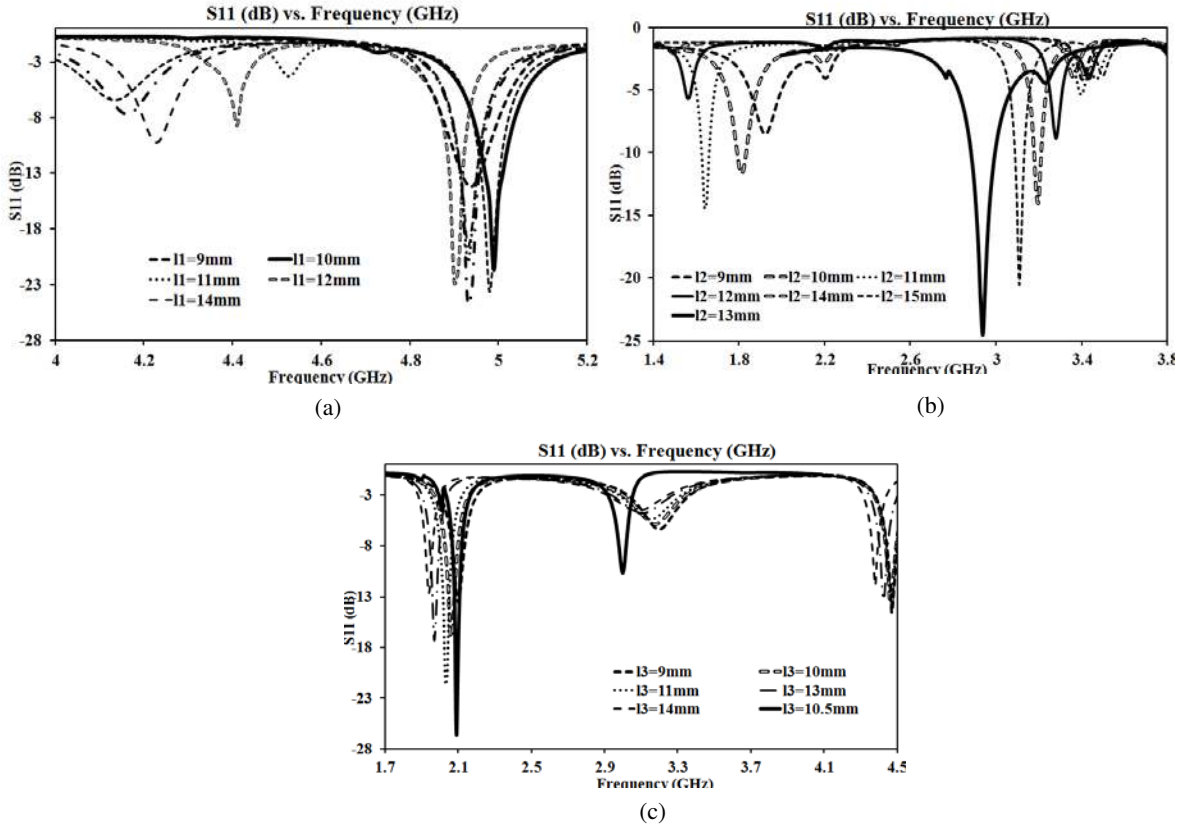

Figure 5. Effect of change in length on S_{11} parameter by (a) stub^1, (b) stub^2, (c) stub^3.

to be completely re-optimized. So to optimize the antenna to achieve the desirable and independent-frequency controls, effect of stub length on the scattering parameter has been studied. Dimension of stub^1 is selected after analyzing the result as shown in Fig. 5(a). Similarly, optimization of stub^2 dimensions is done to get the optimally tuned frequency for stub^2 without affecting the resonating frequency for stub^1 as shown in Fig. 5(b). Finally, matching at third resonant frequency is done by placing stub^3 at the top of feed line, and optimization is done using parametric study as shown in Fig. 5(c). The final selection of dimension for all stubs from parametric study is taken by considering various factors, such as dimensional constraint, unwanted non-resonant sidebands, return loss value at desired frequency, amount of nonlinearity present in the frequency response of return loss, etc. The length chosen for stub^1 is 10 mm, stub^2 13 mm and stub^3 10.5 mm.

3. DESIGN LAYOUT AND EXPERIMENTAL SETUP

The layout of the proposed hybrid antenna for cognitive radio applications consists of a semicircular arc with staircase shape slotted ground structure for wideband operation and a stub-loaded antenna for frequency switching operation. When the hybrid antenna is excited by port^2, the antenna functions as a wideband antenna, and in this case, the antenna is used to scan a very wide spectrum (1 GHz–12 GHz) to check unoccupied spectrum. When the hybrid antenna is excited by port^1, it has four controllable frequency states, i.e., 2.1 GHz, 2.96 GHz, 3.5 GHz and 5 GHz. The proposed hybrid antenna is fabricated on a 1.6 mm thick FR4 substrate (Ws, Ls) with relative permittivity of 4.4 and loss tangent of 0.02. The geometry of the proposed hybrid antenna is presented in Fig. 1. The whole antenna structure is composed of 3 open stubs, 3 PIN diodes (D_1, D_2, D_3), 1 Surface Mount Device (SMD) capacitor, 2 baluns, and 3 biasing pads (V_1, V_2, V_3). The key dimensional parameters of the proposed hybrid antenna are shown in Table 1. The PIN diodes are mounted on the 0.7 mm wide gaps between each stub and the microstrip feed line. DC pads V_1, V_2, and V_3 connected with thin dc bias lines are used to apply the DC voltage to their respective PIN diodes. The feeding lines are thin enough to prevent RF leakage at any frequency in the desired operating regions and behave as a perfect conductor for DC current. The orientations of all PIN diodes are in such a way that these can be biased independently using three different DC voltage pads and share a single ground signal pad V_{gd}. This technique simplifies the biasing scheme by reducing the number of DC ground biasing pads. The balun with $\theta = 60°$ provides a high isolation of RF signal towards DC. SMD capacitor of 30 pF is placed across the 0.5 mm wide gap in the main feed line to maintain RF continuity and DC isolation. The geometrical specifications of semicircular arc with staircase shape slotted ground structure for wideband operation are given in Table 2. The fabricated prototype and experimental setup are shown in Fig. 1(b).

Table 1. Dimension specification (all in mm).

Stub^1	Stub^2	Stub^3	Antenna	Substrate
L_1, W_1	L_2, W_2	L_3, W_3	L_T, W_T	L_s, W_s
10, 2	13, 2	10.5, 2	15, 20	75.6, 66

Table 2. Dimension specification for UWB structure.

$a = 4.5$ mm	$f = 6$ mm	$i = 62$ mm
$b = c = d = 4$ mm	$g = 42$ mm	$j = 2.69$ mm
$e = 2$ mm	$h = 38.15$ mm	

4. DESIGN VERIFICATION THROUGH SIMULATION

4.1. Modelling of PIN Diode

The BAR 64-02 diodes (Size: $1.5 \times 0.7\,\text{mm}^2$) are used to electrically connect/disconnect the matching stubs to the microstrip feed line. In simulation, the effect of PIN diode is incorporated by an equivalent circuit as shown in Fig. 6. As can be seen from Figs. 6(a), (b), in ON state PIN diode is modeled as a resistance of 2.1 Ω and in OFF condition modeled as parallel combination of 3 KΩ resistance and a capacitance of value 0.17 pF. During simulation in HFSS, a strip element of size 0.5 mm × 3 mm is used to represent the PIN diode. This strip is assigned by equivalent circuit of PIN diode using lumped boundary (RLC) condition.

4.2. Simulation Results

When neither of the PIN diodes is biased (case^1) the antenna is matched at 3.5 GHz with return loss value 29 dB as shown in Fig. 7. Simulated response of VSWR and impedance for hybrid antenna are

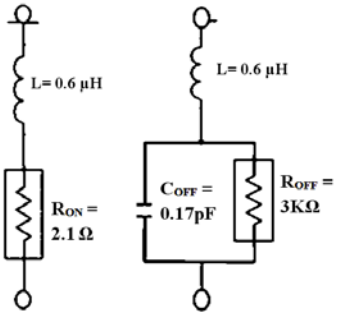

Figure 6. PIN diode equivalent circuit in (a) ON state, (b) OFF state.

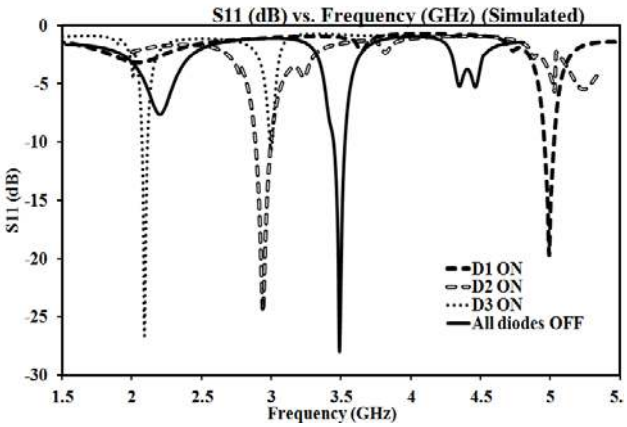

Figure 7. S_{11} vs. freq. for hybrid antenna.

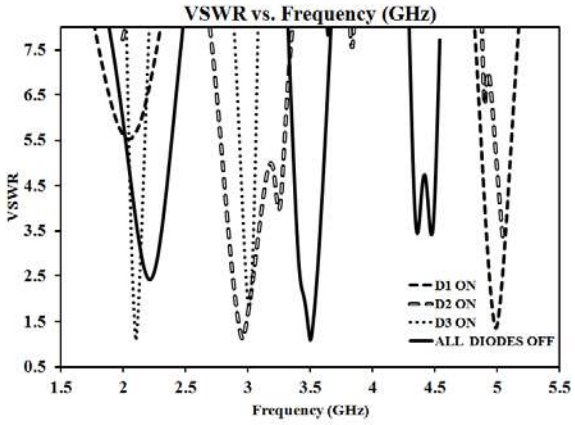

Figure 8. VSWR vs. freq. for hybrid antenna.

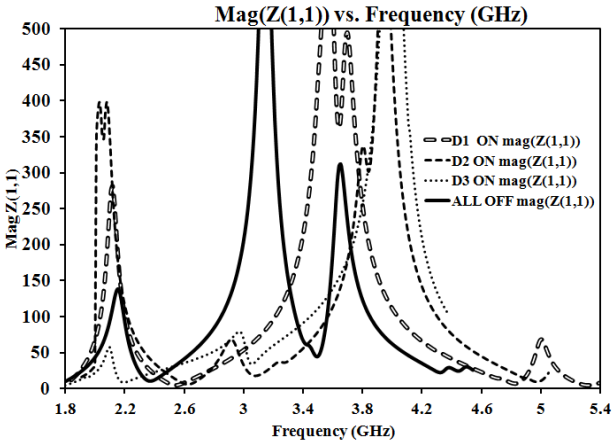

Figure 9. Impedance vs. freq. for hybrid antenna.

given in Figs. 8 and 9 and tabulated in Table 3. In case[2], ON state equivalent circuit is applied to diode D_1 and OFF state equivalent circuit applied to D_2, D_3. In this case, the antenna resonates at 5 GHz with return loss 19 dB, VSWR = 1.349 and impedance = 50.55 Ω. In case[3], when diode D_2 is assigned by its ON state equivalent circuit and other diodes by OFF state equivalents, the antenna is matched to 2.94 GHz with return loss, VSWR and impedance value equal to 25 dB, 1.12 and 51.55 Ω, respectively. Similarly, in case[4], when diode D_3 is replaced by its ON state equivalent, the antenna is matched to 2.1 GHz with return loss, VSWR and impedance value equal to 26 dB, 1.159 and 51.77 Ω, respectively.

4.3. *E* Field Distributions

Figure 10 shows the simulated electric field distributions on the hybrid antenna elements in different switching states. When the hybrid antenna is excited by port[2], the maximum intensity (Red color) of E field extends under the semicircular arc giving rise the wideband response as shown in Fig. 10(a). In frequency reconfiguration mode, for case[1] when all the diodes are OFF, the obtained E field distribution is shown in Fig. 10(b). In case[2], the maximum intensity of electric field extends around the radiating antenna connected with stub[1] as shown in Fig. 10(c). Then in case[3], electric field redistributes, and maximum electric field intensity is found under antenna structure and stub[2], as expected and shown in Fig. 10(d). In case[4], due to the presence of stub[3], the antenna resonates at 2.1 GHz, and the electric field on antenna surface is disturbed and given in Fig. 10(e).

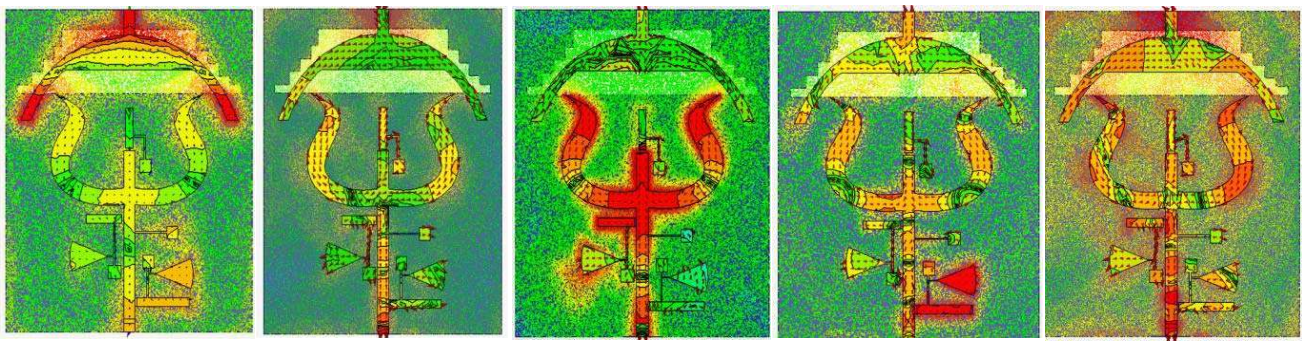

Figure 10. E field distribution under different diode condition. (a) Wideband mode, (b) 3.5 GHz, (c) 5 GHz, (d) 2.96 GHz, (e) 2.1 GHz.

5. EXPERIMENTAL VALIDATION AND DISCUSSION

Switching mechanism and frequency state for each band are explained in this section. For wideband characteristics, the hybrid antenna is excited by port[2], and simulated and measured wideband responses are shown in Fig. 11(a). The impedance matching is optimized by shaping the radiator and controlling the slot shape in the ground plane. The simulated and measured results indicate that return loss is better than −11 dB from 1 to 12 GHz. Hence it can sense the spectrum in the designed UWB range.

When the hybrid antenna is excited by port[1], the hybrid antenna operates in frequency reconfigurable mode. Here, depending on the bias condition of PIN diodes, the antenna operates at any of the four frequencies, i.e., 2.1 GHz, 2.96 GHz, 3.5 GHz and 5 GHz as shown in Fig. 11(b). To select the open stubs, relevant diodes are forward bias by applying +1.1V signal on their respective DC pads and ground signals on V_{gd} pad. In case[1], when all diodes are OFF, the measured value of S_{11} is −26.8 dB at 3.47 GHz compared to the simulated value of −29 dB at 3.5 GHz. There is no significant variation in frequencies in case[1], since all the switches are in OFF state. This results in no loading of antenna, and thereby close agreement is obtained in measured and simulated frequencies. For case[2], when stub[1] is selected by forward biasing diode D_1 the antenna resonates at 4.96 GHz compared to simulated frequency at 5 GHz. The measured value of S_{11} in this case is −22.66 dB compared to simulated value of −33 dB. In case[3], simulated value of return loss is 30 dB at 2.96 GHz whereas measured value of return loss is 27.07 dB at 3 GHz. In the last case, when stub[3] is selected, simulated frequency 2.1 GHz shows the return loss value 37 dB whereas measured value of RL is 35 dB at 2 GHz. The measured results are satisfactory; however, frequency shift w.r.t simulated results are attributed to variation in PIN diodes OFF state capacitance w.r.t to frequency in addition to minor fabrication errors.

Figure 12(a) shows a 3D polar plot for radiation pattern which is bidirectional in elevation plane and omnidirectional in azimuthal plane. Fig. 12(b) shows that maximum gain is 4.8 dB at 20° and 160° in the elevation plane and 4.7 dB in azimuthal plane. The simulated radiation patterns for all reported states have been compared with the measured patterns. Fig. 12(c) shows that in wideband

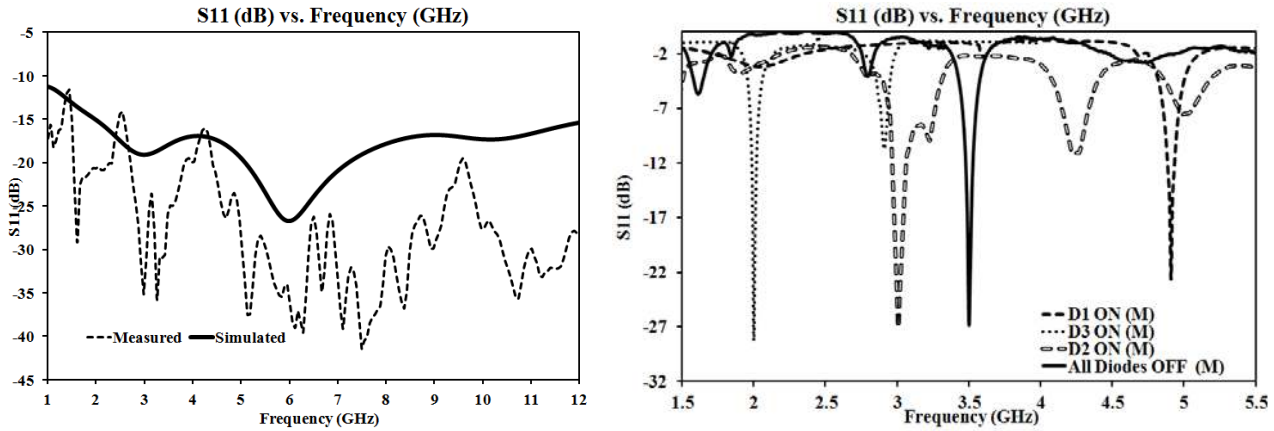

Figure 11. S_{11} vs. frequency of hybrid antenna in (a) wideband mode, (b) frequency reconfigurable mode.

Table 3. Simulated and measured parameter for hybrid antenna.

		Simulated				Measured	
S. No		Freq. (GHz)	S_{11} (dB)	VSWR	Impedance (Ω)	Freq. (GHz)	S_{11} (dB)
Case[1]	All OFF	3.5	−29	1.15	48.794	3.47	−26.8
Case[2]	D_1 ON	5	−19.61	1.35	50.55	4.96	−22.66
Case[3]	D_2 ON	2.96	−24.5	1.12	52.2	3	−27.07
Case[4]	D_3 ON	2.1	−26.56	1.16	51.77	2	−35

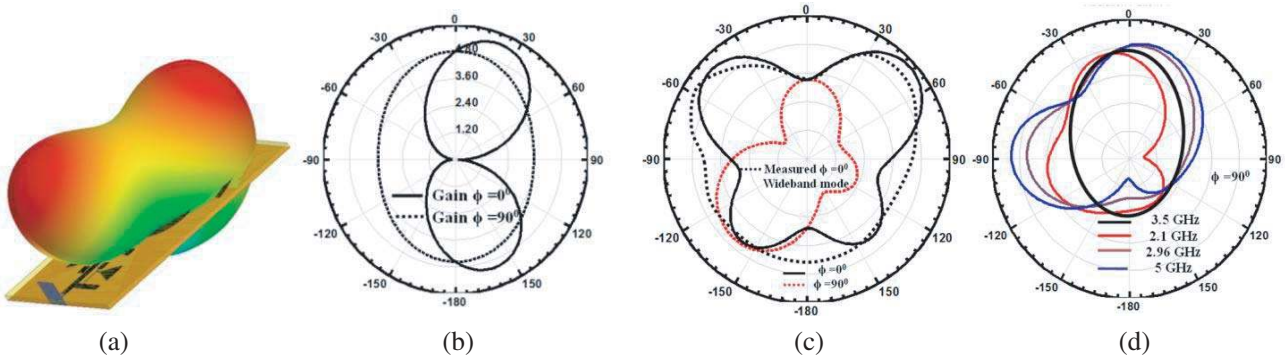

Figure 12. (a) Polar plot for radiation pattern. (b) Gain plot. (c) E and H plane in Wideband mode. (d) H plane for all cases in frequency reconfigurable mode.

mode, the antenna emits well in all the directions in E plane by radiating nearly a circular pattern. In frequency reconfiguration mode simulated H plane patterns for all the cases are omnidirectional as shown in Fig. 12(d). Comparisons of E plane under different diode conditions, i.e., at 3.5 GHz, 5 GHz, 2.96 GHz, and 2.1 GHz are shown in Figs. 13(a)–(d). In case[1], bidirectional pattern having maximum radiation intensity in 20° and 160° direction is observed. In case[2], the obtained structure of pattern is distorted bidirectional with maximum radiation intensity in 40° and −60° directions. In case[3], a perfect doughnut shape pattern having maximum radiation intensity in 10° and 160° is observed. The simulated radiation pattern in case[4] has two sidelobes in −140° and 140° direction and two main lobes

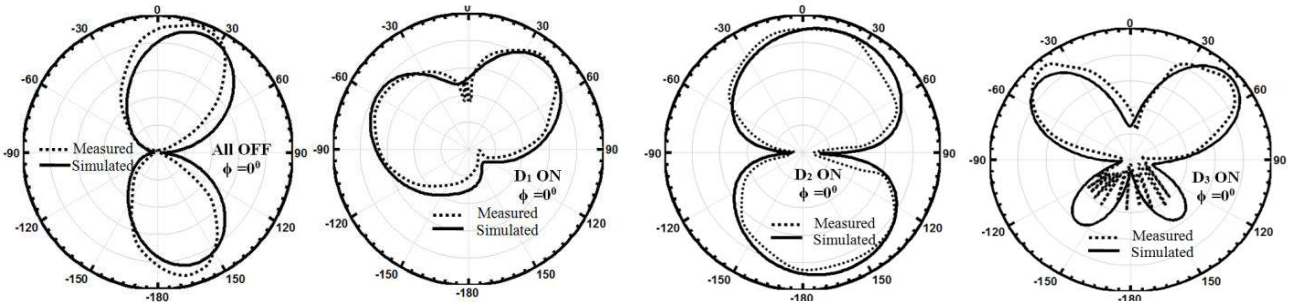

(a) (b) (c) (d)

Figure 13. *E* plane in frequency reconfigurable mode (a) at 3.5 GHz, (b) 5 GHz, (c) 2.96 GHz, (d) 2.1 GHz.

in $-50°$ and $50°$ direction. These sidelobes radiate some part of the total energy which is undesired for efficient radiation. Measured patterns in all the cases are in close agreement with the simulated ones.

6. CONCLUSION

The paper describes a hybrid antenna which can sense the spectrum from 1 GHz–12 GHz using a wideband antenna and after sensing it can reconfigure its frequency in any of the four frequency states — 2.1 GHz, 2.96 GHz, 3.5 GHz and 5 GHz. Simulated and measured results show satisfactory performance. The advantages of the proposed hybrid antenna are that both the modes: wideband and frequency reconfigurable are achieved using a simple, cost effective and compact prototype. Furthermore, all frequency states are achieved electronically and work independently resulting in no interference, hence, the proposed hybrid antenna can be used for CR applications.

REFERENCES

1. Tawk, Y., M. Bkassiny, G. El-Howayek, S. K. Jayaweera, and Avery, "Reconfigurable front-end antennas for cognitive radio applications," *IET Microw. Antennas Propag.*, Vol. 5, No. 8, 985–992, 2011.
2. Haykin, S., "Cognitive radio: Brain-empowered wireless communications," *IEEE Journal on Selected Areas in Communications*, Vol. 23, 201–220, Feb. 2005.
3. Marshall, P., *Quantitative Analysis of Cognitive Radio and Network Performance*, Artech House, 2010.
4. Mansoul, A., F. Ghanem, M. Hamid, and M. Trabelsi, "A selective frequency-reconfigurable antenna for cognitive radio applications," *IEEE Antennas Wireless Propagat. Lett.*, Vol. 13, 2014.
5. Hussain, R. and M. S. Sharawi, "A cognitive radio reconfigurable MIMO and sensing antenna system," *IEEE Antennas Wireless Propagat. Lett.*, Vol. 14, 257–260, 2015.
6. Qin, P.-Y., F. Wei, and Y. J. Guo, "A wideband-to-narrowband tunable antenna using a reconfigurable filter," *IEEE Trans. Antennas Propagat.*, Vol. 63, No. 5, 2282–2285, May 2015.
7. Abutarboush, H. F., R. Nilavalan, S. W. Cheung, K. M. N. T. Peter, D. Budimir, and H. Al-Raweshidy, "A reconfigurable wideband and multiband antenna using dual-patch elements for compact wireless devices," *IEEE Trans. Antennas Propagat.*, Vol. 60, No. 1, 36–43, 2012
8. Sharma, S. and C. C. Tripathi, "Wideband to concurrent tri-band frequency reconfigurable microstrip patch antenna for wireless communication," *Int. Journal of Microw. and Wireless Tech.*, 2016. doi:10.1017/S1759078716000763
9. Elham Ebrahimi, C., J. R. Kelly, and P. S. Hall, "Integrated wide-narrowband antenna for multi-standard radio," *IEEE Trans. Antennas Propagat.*, Vol. 59, No. 7, 2628–2635, Jul. 2011.

10. Hamid, M. R., P. Gardner, P. S. Hall, and F. Ghanem, "Vivaldi antenna with integrated switchable band pass resonator," *IEEE Trans. Antennas Propagat.*, Vol. 59, No. 11, 4008–4015, Nov. 2011.
11. Augustin, G. and T. A. Denidni, "An integrated ultra wide/narrow band antenna in uniplanar configuration for CR systems," *IEEE Trans. Antennas Propagat.*, Vol. 60, No. 11, 5479–5484, 2012.
12. Sharma, S. and C. C. Tripathi, "Frequency reconfigurable U-slot antenna for SDR application," *Progress In Electromagnetics Research Letters*, Vol. 55, 129–136, 2015.
13. Aboufoul, T., A. Alomainy, and C. Parini, "Reconfiguring UWB monopole antenna for cognitive radio applications using GaAs FET switches," *IEEE Antennas Wireless Propagat. Lett.*, Vol. 11, 392, 2012.